B1, a novel HDAC inhibitor, induces apoptosis through the regulation of STAT3 and NF-κB

MENG-HSUAN CHENG[1,2], YUN-HONG WONG[2,3], CHIA-MING CHANG[3], CHUN-CHIEN YANG[2,3], SHIH-HUA CHEN[3], CHUN-LUNG YUAN[4], HSIAO-MEI KUO[5], CHUN-YUH YANG[6] and HUI-FEN CHIU[2,3]

[1]Division of Pulmonary and Critical Care Medicine, Department of Internal Medicine, Kaohsiung Medical University Hospital, Kaohsiung 80756; [2]Graduate Institute of Medicine and [3]Department of Pharmacology, College of Medicine, Kaohsiung Medical University, Kaohsiung 80708; [4]Department of Chemistry, Republic of China Military Academy, Fengshan, Kaohsiung 83059; [5]Department of Neuroscience, Marine Biotechnology and Resources, National Sun Yat-sen University, Kaohsiung 80424; [6]Faculty of Public Health, College of Health Science, Kaohsiung Medical University, Kaohsiung 80708, Taiwan, R.O.C.

Received October 31, 2016; Accepted March 27, 2017

DOI: 10.3892/ijmm.2017.2946

Abstract. We previously demonstrated that B1 induced significant cytotoxic effects, cell cycle G1 arrest and apoptosis in human lung cancer A549 cells through the inhibition of DNA topoisomerase II activity. In the present study, we focused on the histone deacetylase (HDAC) modulation of B1 in A549 cells. HDACs, important enzymes affecting epigenetic regulation, play a crucial role in human carcinogenesis. Our findings showed that B1 could suppress the growth of A549 cells *in vitro* through the inhibition of HDAC activity. Additionally, B1 caused disruption of the mitochondrial membrane potential and induced DNA double-strand breaks (DSBs) in a dose- and time-dependent manner, which consequently led to cell apoptosis. We also observed that B1 inhibited cancer cell migration and angiogenesis-related signal expression, including vascular endothelial growth factor (VEGF) and pro-matrix metalloproteinases-2 and -9 (pro-MMP-2/9). Gelatin zymography suggested that B1 decreased pro-MMP-2 and pro-MMP-9 activity. Transcription factors, signal transducer and activator of transcription 3 (STAT3) and nuclear factor-κB (NF-κB), are vital players in the many steps of carcinogenesis. B1 showed significant dose-response inhibitory effects on cytoplasmic expression and nuclear translocation of both phosphorylated STAT3 (pSTAT3) and NF-κB. It has been well documented that reactivated telomerase confers cancer cells the ability to repair DNA. Real-time PCR results indicated that B1 inhibited STAT3 and NF-κB mRNA expression and telomerase activity. Taken together, our results demonstrated that B1 exerted significant inhibitory effects on HDAC, telomerase activities, oncogenic STAT3 and NF-κB expression. The inhibition of the intricate crosstalk between STAT3 and NF-κB may be a major factor in the molecular action mechanism of B1. The multiple targeting effects of B1 render it a potential new drug for lung cancer therapy.

Correspondence to: Professor Hui-Fen Chiu, Graduate Institute of Medicine, College of Medicine, Kaohsiung Medical University, Kaohsiung 80708, Taiwan, R.O.C.
E-mail: chiu358@yahoo.com.tw

Key words: histone deacetylase inhibitor, signal transducer and activator of transcription 3, nuclear factor-κB, telomerase, matrix metalloproteinase-2

Introduction

B1 is one of hundreds of newly synthesized diamidoanthraquinones in our new drug development plan. B1, which shares its basic structure with commercial anticancer drugs mitoxanthrone and doxorubicin, exhibits more potent cytotoxic effects in human lung, colon and breast cancer cell lines. We previously reported that B1 significantly inhibited DNA topoisomerase II activity and induced apoptosis and cell cycle G1 arrest in human lung cancer A549 cells (1).

Lung cancer remains the most common cause of cancer-related deaths worldwide, and despite global efforts, there has only been marginal improvements in lung-cancer-related morbidity and mortality, and the median survival time of metastatic lung cancer patients is no more than ~1 year (2). Therefore, the development of new small-molecule drugs to treat lung cancer is urgently needed.

Epigenetic and genetic abnormalities are believed to be involved in all stages of cancer development. Epigenetic regulation refers to changes in gene expression without alternation of the DNA sequence. Due to the reversibility of epigenetic modulation, and subsequent downstream aberrant expression of associated proteins in tumor cells, an increasing amount of research has focused on agents that target dysregulated epigenetic pathways (3).

Histone acetylation is one of the most studied pathways of epigenetic regulation, and enzymes, such as histone acetyltransferases (HATs) and deacetylases (HDACs), modulate this regulation. Suberoylanilide hydroxamic acid (SAHA), a commercial HDAC inhibitor (HDACi), has been shown to

upregulate gene expression, including tumor suppressor p21, p53, Fas, Bax and caspases; while downregulating oncogenes, including Bcl-2, XIAP, vascular endothelial growth factor (VEGF), and cyclin D1 (4). However, histones may not be the only substrates of HDACs and HATs. Modifications of non-histone proteins, such as NF-κB, p53 and STAT3, are also important in the regulation of gene expression (5). Currently, the US Food and Drug Administration (FDA) has approved two HDACis, SAHA (also known as vorinostat) and romidepsin, for the treatment of cutaneous T-cell lymphoma (6).

Telomeres, consisting of tandem 6-base subunit (TTAGGG) repeats, are highly specialized nucleic acid protein complexes located at the ends of chromosomes. They protect chromosomes from degradation (7). Activated telomerase maintains essential telomere length, and with the exception of germ line and selected progenitor cells, telomerase activity is undetectable in the majority of somatic cells. However, the reactivation of telomerase is readily detected in 80 to 90% of human malignant tumors, rendering it an attractive target in the development of anticancer agents (8).

The STAT protein family is made up of latent cytoplasmic transcription factors, which participate in uncontrolled proliferation, resistance to apoptosis, maintenance of angiogenesis, and escape from immune surveillance of cancer cells (9). In particular, constitutive STAT3 activation has been found in a variety of solid and hematologic human malignancies, such as lung, breast and prostate cancers (10). STAT3 is the upstream of telomerase and transcription factor NF-κB, both of which play a vital role in tumorigenesis (11,12). NF-κB generally remains silent in the cytoplasm, where it binds with inhibitory IκB proteins. In response to extracellular and intracellular signaling, phosphorylated IκB becomes polyubiquitinated, allowing NF-κB to translocate into the nucleus, which subsequently leads to gene transcription modulation. Aberrant NF-κB signaling can inhibit apoptosis, and induce cell proliferation, migration and invasion, which consequently induces tumor progression (13).

This study focused on a further detailed characterization of B1, including the inhibitory effects of HDAC, pro-matrix metalloproteinases-2 and -9 (pro-MMP-2/9), and telomerase. We also investigated the role of B1 in the induction of DNA double-strand breaks, mitochondrial membrane potential disruption, and its influence on STAT3 and NF-κB nuclear translocation.

Materials and methods

Reagents. B1 was synthesized and supplied by Dr Hsu-Shan Huang at the National Defense Medical Center (Taipei, China). A stock solution of B1 was prepared in dimethyl sulfoxide (DMSO), protected from light, and stored at -20˚C. Fig. 1A shows the chemical structure of B1. Prior to use, the B1 solution was freshly prepared in a medium at the desired concentrations. The tetrazolium reagent (XTT), 3,3-dihexyloxcarbocyanine ($DiOC_6$), HDACis including trichostatin A (TSA) and SAHA, and antibodies for acetyl-histone H3 (#H0913), MMP-2 (#AV20016) and MMP-9 (#SAB1402274) were purchased from Sigma-Aldrich (St. Louis, MO, USA). Anti-Fas (#610197) and anti-Bad (#610392) were purchased from BD Technologies (Research Triangle Park, NC, USA). Antibodies against STAT3 (#9139), phosphorylated STAT3 at Tyr705 (pSTAT3, #9131), Bcl-xL (#2762), Apaf-1 (#5088), HDAC3 (#3949), and histone H3 (#9715) were obtained from Cell Signaling Technology, Inc. (Beverly, MA, USA). Antibodies for glyceraldehyde 3-phosphate dehydrogenase (GAPDH) (#128915) and β-actin (#8229) were purchased from Abcam (Cambridge, UK). Antibodies for VEGF-D (#13085) and NF-κB (p65, #372) were obtained from Santa Cruz Biotechnology, Inc. (Dallas, TX, USA).

Cell lines and cell cultures. Human lung adenocarcinoma cell line (A549), hepatocellular carcinoma cell line (HepG2), and rat glioma cell line (C6) were obtained from the Bioresource Collection and Research Center, Taiwan. The 2.2.15 cell line, a clonal derivative of the HepG2 (ATCC HB8065) cell, was obtained by stable transfection with a plasmid containing head-to-tail hepatitis B virus dimer and selected in a medium containing G418. The 2.2.15 cell line was kindly provided by Professor Yang-Chi Chang, Department of Pharmacology, Yale University (New Haven, CT, USA). All cancer cell lines were cultured with MEM medium supplemented with 10% fetal calf serum and antibiotics (100 U/ml penicillin G and 100 μg/ml streptomycin).

Cell cytotoxicity assay. Cell viability, following treatment with B1 for 72 h, was assessed by XTT assay. Briefly, the different cancer cell lines were plated into 24-well culture plates ($5x10^4$ cells/well), and grown for 24 h. The cells were then treated with various concentrations of B1 for 72 h at 37˚C in a humidified atmosphere containing 5% CO_2. DMSO alone was used as a control. After the desired treatment duration, the cells were collected by brief trypsinization and measured by colorimetric XTT assay as previously described (1). Proliferation rates were obtained from the B1-treated wells, as compared to those in the absence of B1 (100% control value). The data shown in this study are the means of six independent experiments.

Detection of double-strand DNA damage: comet assay. The degree of DNA double-strand breaks (DSBs) was evaluated by alkaline comet single-cell gel electrophoresis. Briefly, $2x10^5$ cells were seeded on 3.5-cm dishes for 24 h and then exposed to various concentrations of B1. After an incubation period, the cells were collected and suspended in cold-phosphate-buffered saline (PBS). Ten microliters of the cell suspension was added to 75 μl of low-melting agarose and immediately pipetted onto the CometSlide (Trevigen, Gaithersburg, MD, USA). After the gel was solidified, the slides were immersed in an ice-cold alkaline lysis solution (Tris-base 10 mM, NaCl 2.5 M and EDTA 100 mM, pH 10) in darkness for 60 min at 4˚C. The slides were then transferred to a horizontal electrophoresis apparatus at 24 V for 20 min, and neutralized by immersing them in Tris-buffer (400 mM, pH 7.5). The cells were then stained with SYBR-Green I (1:10,000) for 10 min in darkness, and images were captured by a fluorescence microscope (Axioskop 2 plus; Zeiss, Thornwood, NY, USA).

Measurement of mitochondrial transmembrane potential. Mitochondrial transmembrane potential ($\Delta\Psi_m$) dissipation was measured using a fluorometric probe,

3,3-dihexyloxcarbocyanine ($DiOC_6$). A549 cells were plated in 3.5-cm dishes, and after reaching confluence, were treated with various concentrations of B1 for 24 h. After incubation, the cells were stained with 40 nM $DiOC_6$ for 30 min at 37˚C, washed with PBS, and analyzed by flow cytometry on a Beckman Coulter Epics XL cytometer (EXPO32XL; Beckman Coulter, Miami, FL, USA). The percentage of cells showing lower fluorescence and reflecting a loss of $\Delta\Psi_m$ were determined by comparison with the untreated controls using Expo32 software.

Terminal deoxynucleotidyltransferase-mediated dUTP nick end labelling (TUNEL) assay. TUNEL assay was carried out using the In Situ Cell Death Detection kit (Fluorescein-Alexa Fluor® 488 Green) according to the manufacturer's instructions (Roche Diagnostics GmbH, Mannheim, Germany).

Wound-healing assay. A wound-healing assay was used to determine the effects of B1 on cell migration. A549 cells ($1x10^7$ cells/well) were seeded into 6-multi-well plates, and grown in medium containing 10% fetal bovine serum (FBS) to a nearly confluent cell monolayer. At confluence, the monolayers were wounded using a micropipette tip, washed twice with PBS, and incubated with various concentrations of B1 for 24 h at 37˚C, and the migrating cells in the wounded area were photographed and counted.

Gelatin zymography. The secreted MMPs by A549 cells were assayed by gelatin zymography. Briefly, the cells were cultured in DMEM, and supplemented with 10% FBS for 24 h. The cells were washed twice with PBS, and incubated with various concentrations of B1 in FBS-free media for 48 h. Then, the conditioned medium was collected, centrifuged and adjusted to the same protein concentration for further gelatinase activity measurement. A 10% polyacrylamide gel was prepared according to the standard procedure, except that it contained 0.1 mg/ml gelatin and the samples were separated under non-reducing conditions. After electrophoresis, the gels were shaken in 2.5% Triton X-100 for 1 h, and then, incubated in 50 mM Tris-HCl buffer (pH 8.0) containing 10 mM $CaCl_2$ and 1 mM $ZnCl_2$ overnight at 37˚C. After the incubation period, the gels were stained with 1% Coomassie Brilliant Blue R-250 for 60 min, and then destained with 10% acetic acid and 40% methanol. The gelatinolytic regions by MMPs became visible against a blue background. Desitometric analysis of the bands, as representative of the relative proteinase activity, was conducted with ImageJ software.

Nuclear and plasma protein separation. After B1 treatment for 48 h, the A549 cells were harvested and resuspended in a cell lysis buffer (10 mM KCl, 10 mM HEPES, pH 7.9, 1.5 mM $MgCl_2$, 1 mM DTT, and supplemented with protease and phosphatase inhibitors), and incubated at 4˚C for 10 min. The lysates were centrifuged at 14,000 x g for 5 min at 4˚C, and the supernatant was collected in order to obtain cytosolic proteins. The pellet (nuclei) fractions were rinsed twice with a washing buffer (10 mM HEPES, pH 7.9, 10 mM $MgCl_2$, 10 mM KCl, 0.5% NP-40, and protease and phosphatase inhibitors), and the supernatant was removed after centrifugation. The nuclear pellets were incubated in a high salt buffer [20 mM HEPES, pH 7.9, 1.5 mM $MgCl_2$, 0.2 mM EDTA, 300 mM NaCl, and 29% (v/v) glycerol], and then protease and phosphatase inhibitors were added. During further western blot analysis, anti-histone H3 and anti-β-actin antibodies were separately used as the loading control for nuclear and cytosolic fractions.

Western blot analysis. Cells were cultured with or without B1 for 48 h, and then both adherent and floating cells were harvested. After being washed with ice-cold PBS and lysed with RIPA reagent (Sigma-Aldrich) for 30 min at 4˚C, the cells were centrifuged at 13,500 rpm for 15 min. Regarding western blotting, equal amounts of total protein were loaded onto glyceraldehyde 3-phosphate dehydrogenase (SDS-PAGE), and the separated proteins were transferred onto a PVDF membrane (Bio-Rad, Hercules, CA, USA). Regarding the blocking of a non-specific binding, the PVDF membrane was soaked in PBS solution containing 5% nonfat milk at room temperature for 1 h. The membranes were probed for migration and apoptosis regulatory protein levels using specific primary antibodies, followed by peroxidase-conjugated appropriate secondary antibodies, which were visualized using enhanced chemiluminescence.

Telomerase activity (real-time quantitative telomeric repeat amplification). The cellular proteins extracted from A549 cells were treated with the indicated concentrations of B1 for 24, 48 and 72 h. An SYBR-Green RTQ-TRAP assay was performed with a dilution of the A549 protein extracts in 25 μl with SYBR-Green PCR Master Mix (Allied Biotech, Inc., Vallejo, CA, USA).

The real-time PCR (ABI 7900 Sequence Detection System) conditions consisted of 25˚C for 20 min for the telomerase reaction, followed by 40 cycles consisting of 95˚C for 30 sec, 60˚C for 30 sec, and 72˚C for 30 sec (3-step PCR). The change in fluorescence intensity (ΔRn) is as shown on the y-axis, and plotted against the cycle number. The telomerase activity was estimated by the cycle threshold (Ct) value.

mRNA isolation and reverse transcription-quantitative PCR (RT-qPCR). Total RNA was extracted from A549 cells with the standard TRIzol reagent (Invitrogen, Carlsbad, CA, USA), following the manufacturer's instructions. An Eppendorf BioPhotometer was used to assess RNA purity and quantity. Five micrograms of total RNA were converted into cDNA using cDNA Reverse Transcription kits (Applied Biosystems, Foster City, CA, USA). Mouse primers for the genes of interest were used for STAT3, 5'-ACCTGCAGCAATACCATTGAC-3' (forward) and 5'-AAGGTGAGGGACTCAAACTGC-3' (reverse); NF-κB (p65), 5'-CGAATGGCTCGTCTGTAGT GCA-3' (forward) and 5'-TGCGCTGACTGATAGCCTGCT CCAGGT-3' (reverse); and GAPDH, 5'-CTCTCTGCTCCTCC TGTTCGAC-3' (forward) and 5'-TGA GCGATGTGGCTC GGCT-3' (reverse). The housekeeping gene GAPDH was used as an internal control. The quantitative PCR (qPCR) reaction used 200 nM forward/reverse primer, 20 ng of cDNA, and Power SYBR-Green PCR Master Mix (Applied Biosystems) in a final volume of 25 μl. PCR was conducted using the StepOnePlus Real-Time PCR system (Applied Biosystems) under the following cycling conditions: 95˚C for 10 min, 40 cycles of 95˚C for 15 sec, and 60˚C for 1 min. All PCR reactions were analyzed in triplicate. The cycle threshold (Ct)

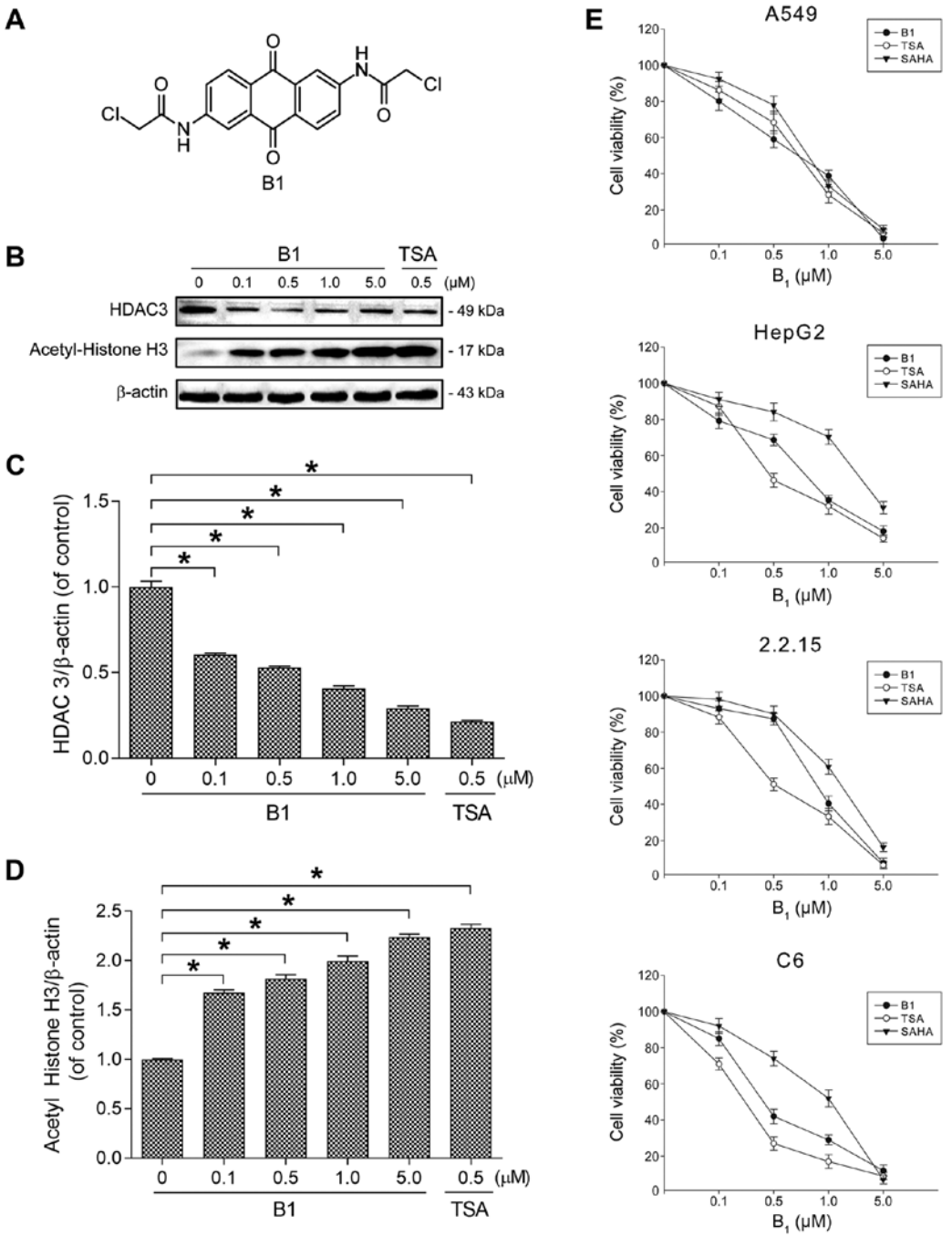

Figure 1. Chemical structure, cytotoxicity, and the effect of histone H3 acetylation of B1. (A) Structure of B1 [2,6-bis-(2-chloroacetamido) anthraquinone]. (B) A549 cells were treated with the indicated concentrations of B1 and TSA for 48 h. The cell lysates were examined for the expression of histone deacetylase 3 (HDAC3), acetylated histone H3, and β-actin by western immunoblot analysis. (C and D) The levels of HDAC3 and acetylated histone H3 were determined by immunoblotting, followed by quantitative analysis using ImageJ software. The data were normalized to β-actin level. (E) Dose-response effects of B1 on cell growth in various cancer cell lines. The cells were treated with different concentrations of B1 for 72 h, and cell viability was determined by XTT assay. Each point represents the mean values ± SE of at least six independent experiments (*P<0.05).

method was used to quantificatively detect PCR products. The relative expression of STAT3 and NF-κB mRNA levels were normalized using GAPDH as the endogenous housekeeping control.

Statistical analysis. Quantitative data were assessed using the Student's t-test, where values are representative of at least three separate experiments with reproducible results. A P-value of <0.05 was regarded as being indicative of statistical significance

Results

Effect of B1 on histone acetylation in A549 cells. The effect of B1 on histone acetylation was examined by western blotting with TSA, as the positive control. Fig. 1B shows that the incubation of A549 cells, with increasing concentrations of B1 for 48 h, significantly decreased the expression of HDAC3 and induced the accumulation of acetylated histone H3. Significant (P<0.05) change in HDAC3 and acetylated histone H3 was noted after 48 h of 0.1 μM B1 treatment (Fig. 1C and D).

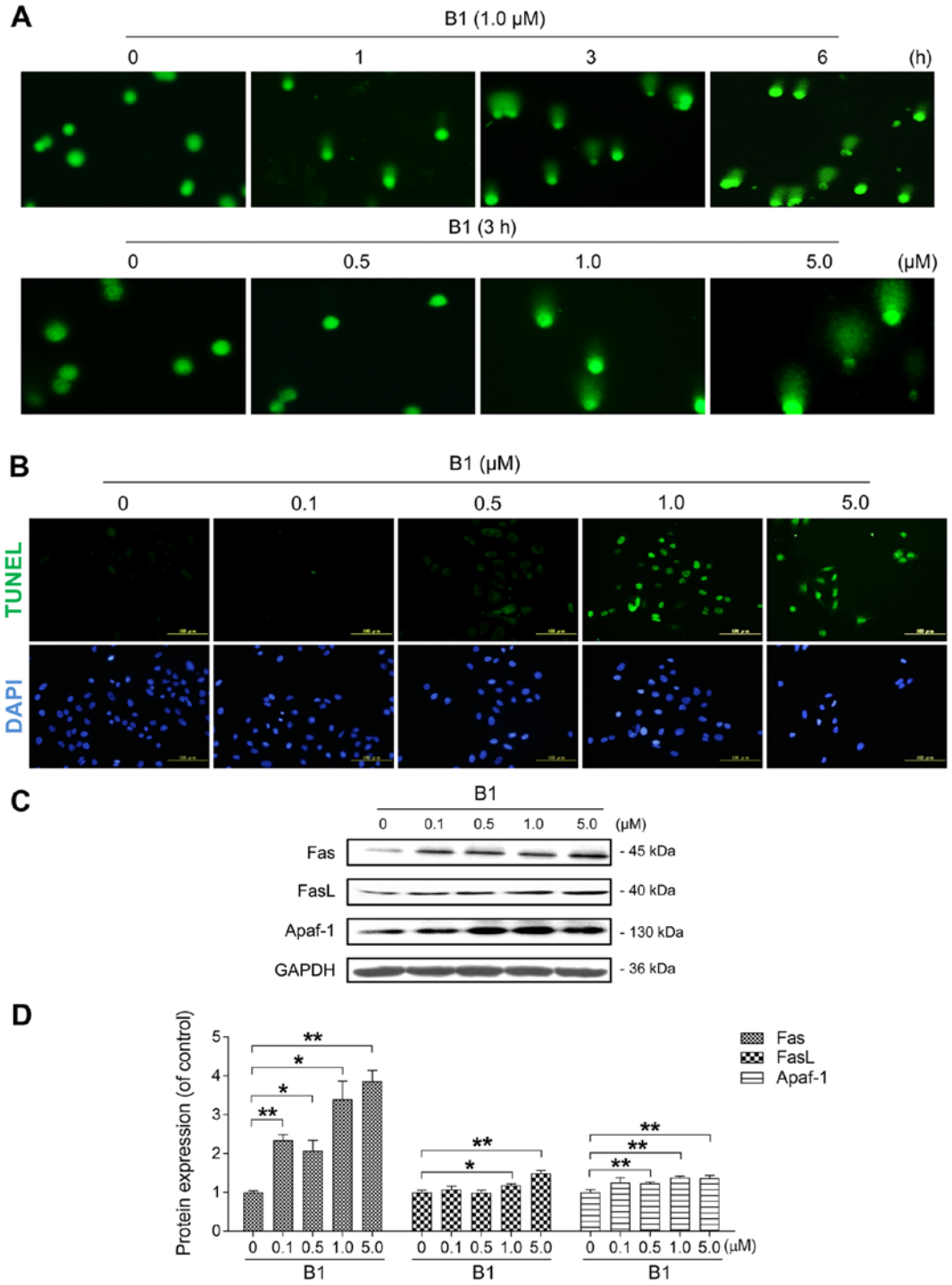

Figure 2. B1 treatment induces DNA damage and apoptosis in A549 cells. (A) Comet images of DNA double-strand breaks were obtained in cells treated with 1.0 μM B1 at various time intervals (x100), or with the indicated concentrations of B1 for 3 h (x200). (B) A549 cells were exposed to different concentrations of B1 for 24 h, and apoptosis was determined with terminal deoxynucleotidyltransferase-mediated dUTP nick end labelling (TUNEL) staining, followed by fluorescence detection. (C) Western blot analysis was used to detect apoptosis regulatory proteins in A549 cells treated with various concentrations of B1 for 48 h. (D) Protein expression of Fas, FasL and Apaf-1 after normalization against GAPDH. The data are expressed as the mean ± SE for three independent experiments with similar results. *P<0.05 and **P<0.01 vs. controls.

Cytotoxicity of B1 in various cancer cell lines. As B1 showed HDAC inhibitory activity in our preliminary study, we further determined its cytotoxic effect on various cancer cell lines in comparison with the well-known HDACis, TSA and SAHA. A 72-h treatment with B1 showed potent antiproliferative effects in a dose-dependent manner (Fig. 1E). The effective doses of the tested compounds that inhibited 50% of cell growth (IC_{50}) of the A549 cell line were 0.57 μM for B1, 0.86 μM for SAHA, and 0.62 μM for TSA. The IC_{50} value of B1 was 0.6 μM for HepG2 cells, 0.71 μM for 2.2.15 cells, and 0.47 μM for C6 cells.

DNA DSBs in the B1-treated A549 cells. Our previous research showed that B1 can inhibit topoisomerase II activity (1);

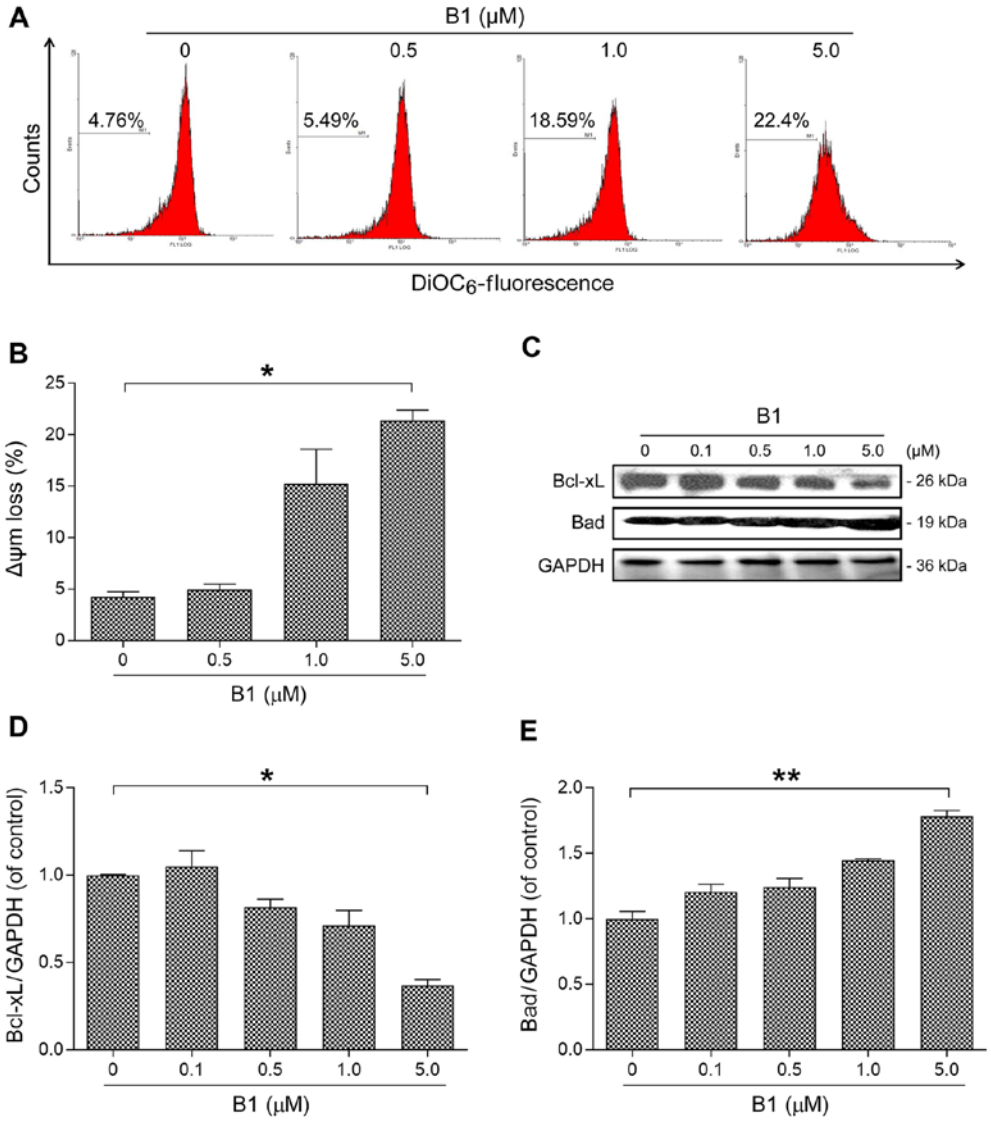

Figure 3. Effect of B1 on mitochondrial membrane potential and associated regulators. (A) A549 cells treated with indicated concentrations of B1 for 24 h were stained with $DiOC_6$ and analyzed by flow cytometry. (B) B1 treatment induced a dose-dependent increase in the proportion of cells with disruption of mitochondrial membrane potential. $^{*}P<0.05$ vs. the untreated control. (C) Western immunoblot analysis of mitochondrial membrane potential-related proteins, Bcl-xL, and Bad, in A549 cells treated with B1 for 48 h. (D and E) Densitometric analysis of three independent western blot analyses revealed relative quantitation of Bcl-xL and Bad levels after normalization against β-actin. $^{*}P<0.05$ and $^{**}P<0.01$ vs. control group.

therefore, the comet assay was performed to elucidate the DNA DSBs caused by B1 treatment. DNA DSBs were observed as having a time-dependent increase in the 1.0 μM B1-treated groups (Fig. 2A). Furthermore, treatment of B1 for 3 h increased DSBs in a concentration-dependent manner.

B1 markedly induces apoptotic cell death by regulating related proteins. HDACis are potent and selective inducers of apoptosis in tumor cells. To further explore the cytotoxic molecular mechanism of B1, we examined the effect of B1 on the apoptosis induction of the treated A549 cells by TUNEL assay. A 24-h treatment of A549 cells with various concentrations of B1 caused an obvious increase in the number of apoptotic cells (Fig. 2B). After engaging with the death receptor Fas, FasL initiates the extrinsic apoptosis pathway. Our data showed that B1 significantly increased the expression of Fas, FasL and Apaf-1 in a dose-dependent manner (Fig. 2C and D).

B1 induces apoptosis via disruption of mitochondrial membrane potential. Depolarization of the mitochondrial membrane potential is one of the earliest characteristic events of apoptosis (14). To test the effects of B1 on mitochondrial membrane potential, A549 cells were stained with $DiOC_6$, a mitochondrial-sensitive dye, following flow cytometric analysis. By interacting with the pro-apoptotic Bcl-2 family members, anti-apoptotic Bcl-2 family proteins regulate the intrinsic apoptotic pathway by modulating mitochondrial membrane potential, and thereby, determining cell death fate by apoptosis (15).

Our results demonstrated that B1 treatment disrupted mitochondrial membrane integrity in a dose-dependent manner (Fig. 3A and B); meanwhile, anti-apoptotic Bcl-xL expression was decreased with a concomitant increase in pro-apoptotic Bad expression, as compared with the untreated control (Fig. 3C-E).

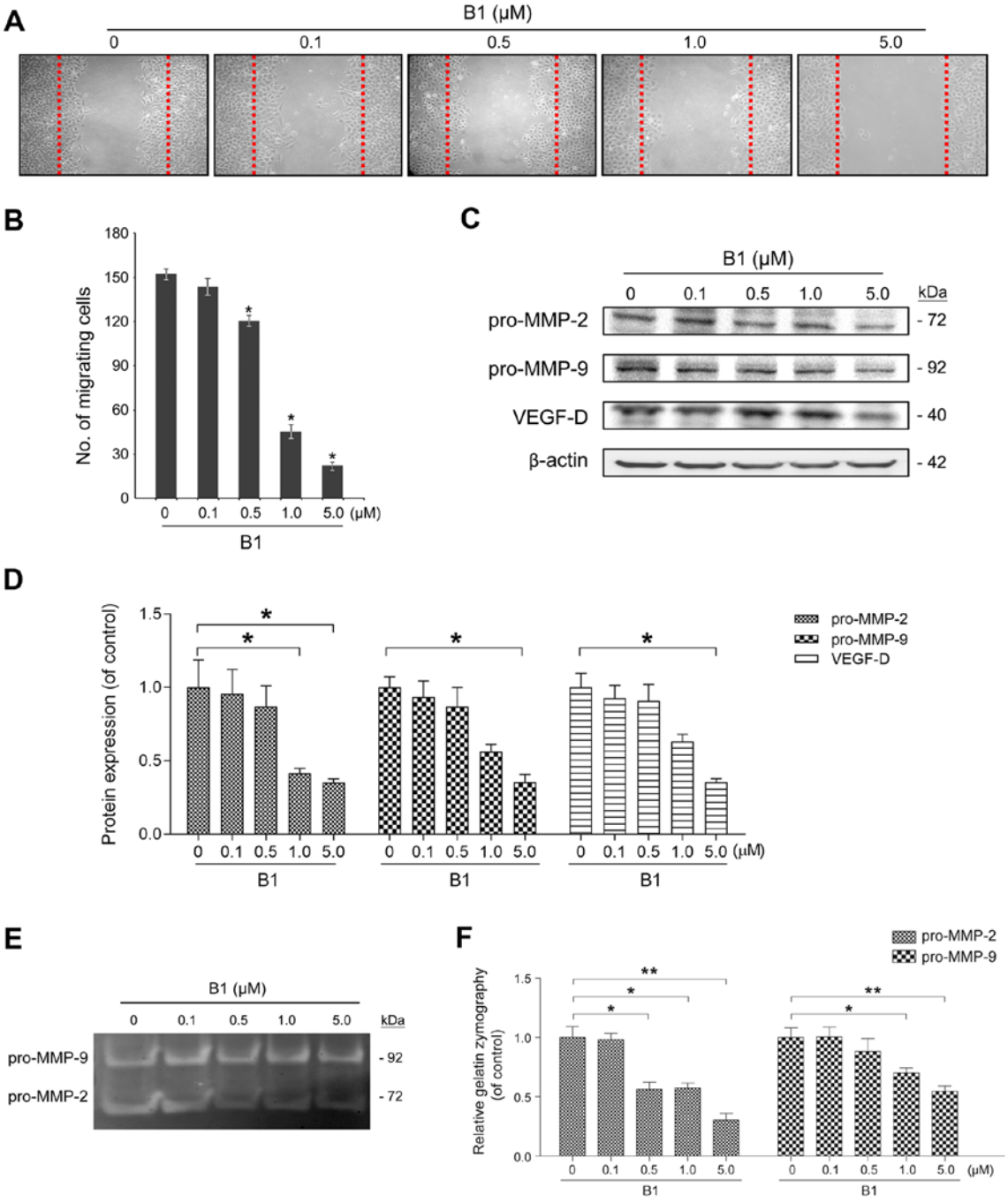

Figure 4. B1 inhibits A549 cancer cell migration, pro-matrix metalloproteinase-2 and -9 (pro-MMP-2/9) expression and activities. (A) A wound-healing assay was performed to evaluate the inhibitory effects of various concentrations of B1 for 24 h. The representative images show the same area after 24 h of incubation with and without different concentrations of B1. (B) Results from three independent experiments are presented as the numbers of migrated cells. *P<0.05, statistically significant compared with the untreated control. (C) The effects of B1 on the expression of migration-related proteins in A549 cells treated with B1 for 48 h. The differential expression of pro-MMP-2/9 and vascular endothelial growth factor (VEGF)-D was assessed by western blot analysis and β-actin was used as a loading control. (D) Densitometric analysis of pro-MMP-2/9 and VEGF-D show the relative quantitation results after normalization against β-actin. *P<0.05 vs. the untreated control. (E) A549 cells were treated in the absence and presence of various concentrations of B1 for 48 h in serum-free medium. The conditioned media were collected for the measurement of pro-MMP-2/9 activity with gelatin zymography, and the (F) bar chart reveals pro-MMP-2/9 activity change after B1 treatment. *P<0.05 and **P<0.01 vs. control group. Data from three independent experiments were presented as mean ± SE.

B1 suppresses the cell migration and inhibits VEGF and pro-MMP-2/9 signaling. The effect of B1 on cancer cell migration was examined using a wound-healing assay. B1 treatment for 24 h significantly inhibited A549 cell migration in a dose-dependent manner (Fig. 4A and B). Similar results were observed in HepG2 and C6 cells (data not shown), indicating that this inhibition phenomenon was neither coincidental nor cell specific.

MMPs, especially MMP-2/9, degrade the extracellular matrix and are crucial for cancer cell movement. VEGF is the most potent inducer of angiogenesis, which plays a vital role in tumor progression and metastasis (16). This study examined

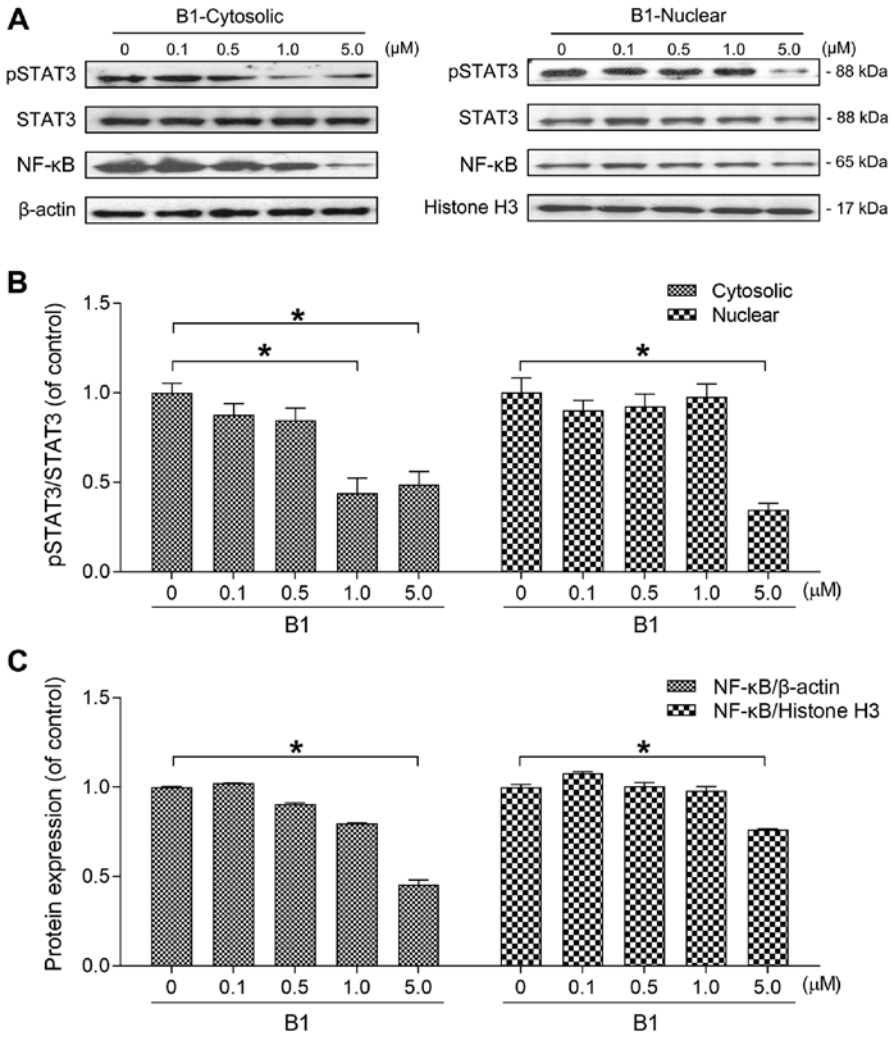

Figure 5. B1 effectively inhibits cytoplasmic, nuclear signal transducer and activator of transcription 3 (STAT3) phosphorylation, and nuclear factor-κB (NF-κB) expression. (A) A549 cells were treated with various concentrations of B1 for 48 h. The cytoplasmic and nuclear protein fractions were separately isolated, and subjected to western blot analysis. The membrane was probed with anti-phosphorylated STAT3 at Tyr705 (pSTAT3), total STAT3, and NF-κB p65 antibodies. The β-actin was used as the loading control for the cytoplasmic fraction and histone H3 for the nuclear fraction. (B) The cytoplasmic and nuclear pSTAT3/STAT3 ratios were analyzed by ImageJ software and normalized to the untreated control. (C) Results of the cytoplasmic and nuclear NF-κB protein expression were separately normalized against β-actin and histone H3. Results are presented as the mean ± SE of triplicate experiments ($^*P<0.05$).

the effects of B1 on the expression of pro-MMP-2 (72 kDa), pro-MMP-9 (92 kDa), and VEGF-D using western blot analysis. Incubation with different concentrations of B1 for 48 h caused a dose-dependent decrease in the expressions of pro-MMP-2/9 and VEGF-D (Fig. 4C and D). Further gelatin zymography examination revealed that B1 treatment for 48 h caused a significant decrease in secreted pro-MMP-2/9 activity (Fig. 4E and F).

B1 inhibits both cytoplasmic and nuclear STAT3 phosphorylation and NF-κB protein expression. Two transcription factors, STAT3 and NF-κB, play a fundamental role in carcinogenesis, and are promising targets for anticancer drug development (17). To elucidate whether the anticancer effects of B1 are associated with STAT3 and NF-κB inhibition, this study examined the expression of the two transcription factors in both the cytoplasm and the nucleus.

The cytoplasmic and nuclear contents were separately extracted and subjected to western blot analysis after A549 cells were treated with various concentrations of B1 for 48 h. The results showed that the expression levels of both cytoplasmic/nuclear phosphorylated STAT3 were attenuated by B1 (Fig. 5A and B).

Since the target genes of NF-κB have been reported to play important roles in tumorigenesis, including proliferation, inflammation, migration and invasion (17), this study also determined the cytoplasmic and nuclear levels of NF-κB. Western blot analysis of nuclear/cytoplasmic proteins revealed that B1 also inhibited NF-κB expression in both compartments (Fig. 5A and C).

B1 inhibits the NF-κB and STAT3 mRNA expression and telomerase activity in A549 cells. To determine whether downregulation of NF-κB and STAT3 proteins after B1 treatment are associated with decreased mRNA expression, this study performed RT-qPCR analysis. B1 treatment significantly decreased mRNA expression of both transcription factors in a dose-dependent manner, and 5.0 μM B1 treatment for 48 h in A549 cells downregulated the STAT3 mRNA level by 40% (Fig. 6A and B).

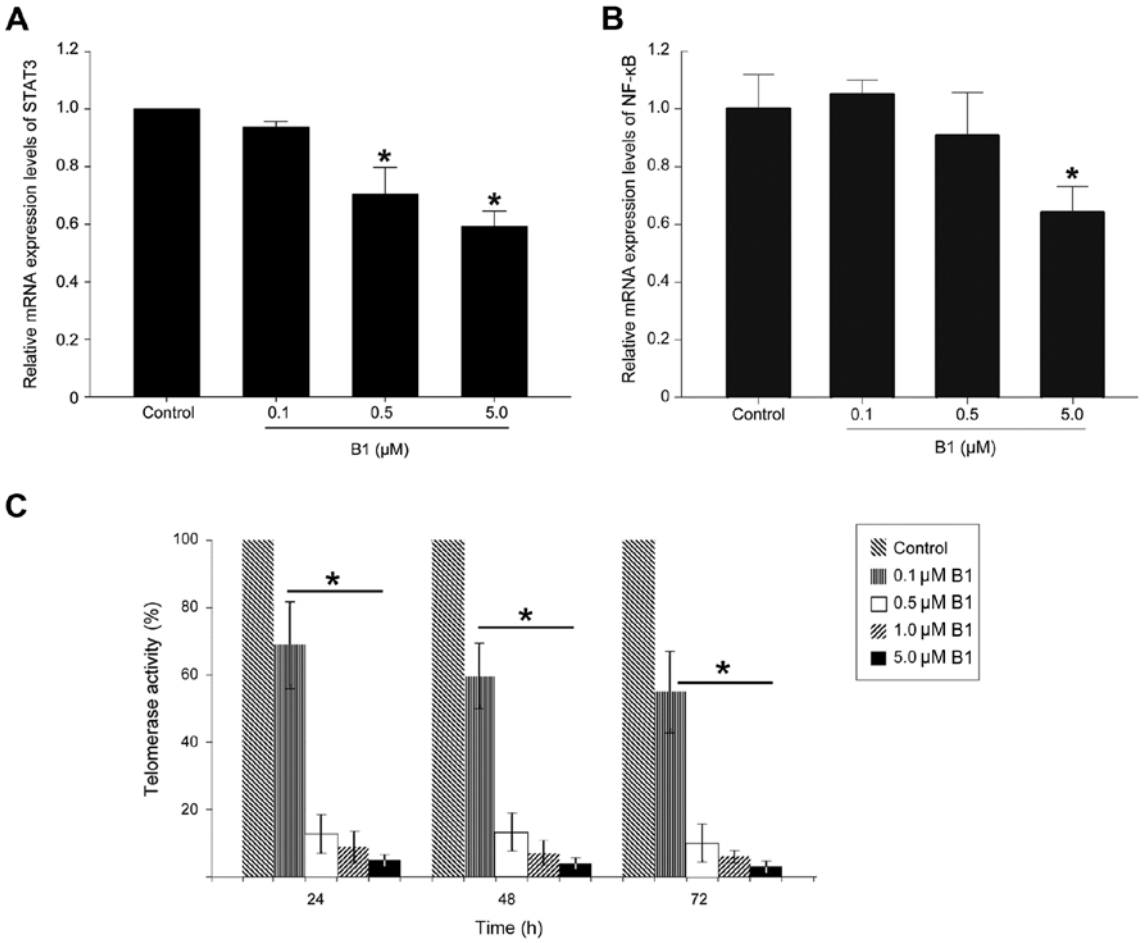

Figure 6. Effects of B1 on nuclear signal transducer and activator of transcription 3 (STAT3) and nuclear factor-κB (NF-κB) mRNA expression and telomerase activity. (A) STAT3 mRNA expression. (B) NF-κB mRNA expression. A549 cells were treated with B1 for 48 h, and the expression of mRNA of both transcription factors was determined by RT-qPCR. The histogram represents the ratios of STAT3 mRNA to GAPDH mRNA, and are shown as the mean ± SE. (C) After treatment with the indicated concentrations of B1 for 24, 48 and 72 h, the telomerase activity of the A549 cells was analyzed by real-time PCR, and expressed relative to the untreated control. Significantly different ($^{*}P<0.05$) compared with the untreated cells.

Recent studies have demonstrated that, in addition to its role in telomere maintenance, telomerase possesses extra-telomeric functions, such as promoting cell proliferation, enhancing DNA-damage repair, and protecting cancer cells from apoptosis (12). As STAT3 has been reported to regulate telomerase activity, and since silencing of STAT3 could effectively downregulate telomerase expression (18) accordingly, we performed a telomerase repeat amplification assay to analyze the effect of B1 on the telomerase activity in A549 cells. The results revealed that the treatment of A549 cells with various concentrations of B1 for up to 24 h showed a significant inhibitory effect on telomerase activity in a time- and dose-dependent manner (Fig. 6C).

Discussion

In our previous study, the newly synthesized 2,6-diamidoanthraquinone derivative, B1, demonstrated potent cytotoxic effects in human lung, colon and breast cancer cells. The antiproliferative mechanism of B1 in human lung cancer cells may act through the induction of cell apoptosis and cell cycle G1 arrest. Moreover, B1 also showed an inhibitory effect on topoisomerase II activity (1).

The present study found that the cytotoxic effects of B1 were not only restricted to the aforementioned human cancer cells, but were also observed in human hepatoma cells (HepG2 and 2.2.15), and in rat glioma cells (C6). Among all human cancer cell lines tested, the human lung cancer cells were more susceptible than the others to the cytotoxic effect of B1. In addition, the growth inhibitory effect of B1, a novel HDACi, was determined to be stronger than the commercial compound SAHA, but weaker than TSA (Fig. 1E).

The aberrant expression or activity of HATs and HDACs has been reported in various cancer cells, and treatment with HDACi has been shown to result in differentiation, cell cycle arrest, inhibition of angiogenesis, and induction of the apoptotic machinery (19). To date, 18 human HDACs with different functions have been identified (20). Among these, HDAC3 may be the key target of vorinostat and romidepsin, the currently available HDACis for the treatment of human cancer (21). Our examination of the effect of B1 on histone acetylation revealed that B1 effectively enhanced the acetylation of histone H3 and inhibited the expression of HDAC3 (Fig. 1B).

Since topoisomerase II inhibitors have been reported to induce apoptosis through the initiation of DNA damage (22), the comet assay was used to determine the DNA damage

caused by B1. The results showed that B1 obviously induced DNA DSBs along with increased treatment time and concentrations (Fig. 2A). Recent research has shown that HDAC3 is involved in DNA damage repair, and that deletion of HDAC3 effectively decreases the DNA damage repair ability (23). Thus, in addition to the topoisomerase II inhibitory effect, DNA DSBs induced by B1 may be mediated, at least in part, through inhibition of HDAC3. Apoptosis induction plays a vital role in HDACi-induced cancer cell death. Our data revealed that TUNEL-positive cells were markedly increased by 0.5 μM B1 treatment for 24 h (Fig. 2B). This result was further supported by the expression changes of the external apoptotic pathway regulators (Fig. 2C and D).

Mitochondrial membrane potential dissipation is essential for the initiation of the internal apoptotic pathway, and is also known as the point of no return for apoptosis. Through modulation of mitochondrial transmembrane potential, the oncoprotein Bcl-2 family controls a crucial point in the regulation of apoptosis. In contrast, Bcl-xL inhibits the formation of lethal Bax/Bak pores on mitochondrial outer membranes, and subsequently prevents apoptosis. The anti-apoptotic proteins, Bcl-2 and Bcl-xL, can be neutralized by the pro-apoptotic protein Bad (24). The major cytotoxic effect of HDACis is mediated through the modulation of the proapoptotic and antiapoptotic proteins of the Bcl-2 family, leading to activation of the intrinsic apoptotic pathway (25). In line with previous studies, we demonstrated that B1 effectively dissipated mitochondrial membrane integrity, and these results were further supported by an increase in Bad and a decrease in Bcl-xL expression in western blot analysis (Fig. 3).

Metastasis causes 90% of cancer-related deaths. Before intravasating into the blood and colonizing in distant organs, the degradation of the extracellular matrix is indispensable to metastatic cancer cells. MMPs are a family of zinc-dependent endopeptidases with the ability to destroy the extracellular matrix; therefore, they play a vital role in cancer invasion and metastasis. In addition, they are involved in different hallmarks of cancer cells, including the promotion of angiogenesis and proliferation, resistance to apoptosis, and escape of immune surveillance (26). Most MMPs are secreted as pro-enzymes (pro-MMPs) or zymogens, and become activated under certain extracellular environments (27). Among these enzymes, MMP-2 and MMP-9, which have the ability to degrade collagen IV, the major component of the basement membrane, are highly expressed in aggressive cancers. Compared with MMP-9, which is induced by specific stimulating factors, MMP-2 is constitutively activated in metastatic tumor cells. The increased expression of MMP-2 was found in human lung tumor samples with more aggressive disease (28). Therefore, targeting MMP-2 could be more important for the treatment of cancer metastasis (29). Our results revealed that B1 inhibited cell migration, pro-MMP-2/9 expression, and their activities in A549 cancer cells (Fig. 4).

The STAT3 transcription factor remains latent in the cytoplasm, and is activated in response to cytokines and growth factor stimuli. These extracellular signals activate receptor tyrosine kinases and non-receptor tyrosine kinases that phosphorylate monomeric STAT3 in the cytoplasm, and subsequently these phosphorylated STAT3 translocate to the nucleus for their transcriptional activities. It has been well established that STAT3 plays an important role in the development and promotion stage of carcinogenesis (30).

NF-κB pathway activation participates in oncogenesis by inhibiting apoptosis, stimulating proliferation, generating tumor-promoting immune activity, and boosting migration and invasion. In mouse models of colitis-associated cancer, inhibition of NF-κB through the deletion of IKKβ in intestinal mesenchymal cells, decreased the incidence and growth of cancer (11), and the same phenomenon has been observed in hepatoma and breast cancer (31,32). In addition to the individual carcinogenesis activity of NF-κB and STAT3, the interaction between these two transcription factors plays vital roles in the control of the communication between malignant cells and the surrounding tumor microenvironment, especially with immune/inflammatory cells (33).

It is now clear that histones are not the only targets of HDACis. In fact, the anticancer effects of HDACis are also achieved through modulation of the acetylation status of many non-histone proteins, including transcription factors, for example, NF-κB, STAT3 and p53 (34). There are studies that HDACis suppress cancer cell growth through the inhibition of STAT3 activation (35,36). In addition, Chien *et al* demonstrated that an HDACi suppressed the growth of pancreatic cancer cells through the inhibition of the NF-κB pathway (37). In concordance with these studies, herein we demonstrated that B1 effectively downregulated cytoplasmic and nuclear pSTAT3/STAT3 ratios and NF-κB expression (Fig. 5). STAT3 has been reported to extend the nuclear retention of NF-κB (38). Therefore, further studies are needed to determine whether the decrease in the nuclear NF-κB protein level after B1 treatment occurs via the inhibition of nuclear translocation and/or via the downregulation of STAT3 expression.

Targeted therapy with epidermal growth factor receptor (EGFR) tyrosine kinase inhibitors (TKIs), erlotinib and gefitinib, showed great efficacy in treating patients with metastatic non-small cell lung cancer harboring EGFR mutations. Human lung cancer cell lines with activating EGFR mutations have shown marked STAT3 activation; however, targeting EGFR mutations cannot effectively inhibit STAT3 activation. In addition, treating cancer cells with EGFR inhibitors can activate the IL-6/JAK/STAT3 signaling pathway, which in turn, induces resistance to these agents (39). The combination of EGFR and STAT3 inhibition has been reported to cause a greater decrease in STAT3 activity and lung cancer growth *in vivo* than either single agent alone (40). At present, traditional chemotherapy is still utilized as the main therapy for patients suffering from EGFR wild-type non-small cell lung cancer; however, its effect is disappointing. Experiments using *in vitro* EGFR wild-type lung cancer cell lines and *in vivo* animal models show that the combination of an HDACi and EGFR-TKI can significantly inhibit the growth of lung cancer cells, which were originally resistant to EGFR-TKI treatment (41). Therefore, B1, with the inhibition of HDAC and STAT3 phosphorylation, could have the potential to be an additive agent together with EGFR-targeted therapy for the treatment of lung cancer, with or without EGFR mutation.

Telomeres, which are located at the end of chromosomes, protect linear chromosomes from degradation. Cells lose 25-200 base pairs of telomeric DNA progressively during each cell generation, and this explains why normal human

somatic cells show a limited replicative life-span during extended culture *in vitro*. Almost all types of malignant cells can maintain telomere length, and most achieve this through upregulation of telomerase activity (42). Telomerase, acting as the central regulator of all the hallmarks of cancer, is reactivated in 90% of all human cancers (43). Telomerase is a downstream target of STAT3, and inhibition of STAT3 through RNA interference has been shown to be sufficient to downregulate the expression of telomerase (18). Previous studies also revealed that HDACis reduce the activity of the catalytic subunit of telomerase (44,45). In line with these studies, our results showed that B1 (which has HDAC and STAT3 inhibitory effects) induced profound suppression of telomerase activity (Fig. 6C).

Currently, the resistance of cancer cells to HDACis is regarded as one of the causes for the disappointing results of the clinical application of HDACis. Recent research has demonstrated that the acetylated STAT3- and DNA methyltransferase 1-mediated activation of insulin-like growth factor 2 transcription and downstream type 1 insulin-like growth factor receptors are important for lung cancer cell lines to become resistant to HDACis (46-48). Furthermore, HDACis revealed significantly antiproliferative activities against both liquid and solid tumor cell lines. Animal studies demonstrated that the toxic effects of HDACis are very weak. Despite this, the FDA has approved HDACis alone for the treatment of liquid tumors, and patients receiving HDACi therapy may still show side effects of traditional chemotherapy, such as diarrhea, fatigue and bone marrow inhibition. It is believed that the reason for the difference between animal studies and clinical trials is that most HDACis inhibit all HDACs, without specific and selective inhibition of HDACs (49). Therefore, the types of the HDACs inhibited by B1 and the *in vivo* anticancer activity will be the focus of our future research.

Cancer is a multi-genetic disease that results from complicated dysregulated biochemical pathways. Therefore, the inhibition of a single signaling pathway by targeted therapy may not provide significant therapeutic benefits and instead, could increase the risk of drug resistance; however, a small molecular anticancer drug with multiple targets may be more beneficial (50). B1 has the ability to inhibit HDAC, telomerase and topoisomerase II, and thus, may be a candidate for future drug development.

Acknowledgements

This study was supported by a grant from the National Science Council, Taiwan (NSC, 99-2320-B037-020-MY3). We appreciated the drug provided by Dr Hsu-Shan Huang, School of Pharmacy, National Defense Medical Center, Taipei.

References

1. Cheng MH, Yang YC, Wong YH, Chen TR, Lee CY, Yang CC, Chen SH, Yang IN, Yang YS, Huang HS, *et al*: B1, a novel topoisomerase II inhibitor, induces apoptosis and cell cycle G1 arrest in lung adenocarcinoma A549 cells. Anticancer Drugs 23: 191-199, 2012.
2. Cataldo VD, Gibbons DL, Pérez-Soler R and Quintás-Cardama A: Treatment of non-small-cell lung cancer with erlotinib or gefitinib. N Engl J Med 364: 947-955, 2011.
3. Pande V: Understanding the Complexity of Epigenetic Target Space. J Med Chem 59: 1299-1307, 2016.
4. Marks PA: Discovery and development of SAHA as an anticancer agent. Oncogene 26: 1351-1356, 2007.
5. Singh BN, Zhang G, Hwa YL, Li J, Dowdy SC and Jiang SW: Nonhistone protein acetylation as cancer therapy targets. Expert Rev Anticancer Ther 10: 935-954, 2010.
6. Duvic M: Histone deacetylase inhibitors for cutaneous T-cell lymphoma. Dermatol Clin 33: 757-764, 2015.
7. Xu L, Li S and Stohr BA: The role of telomere biology in cancer. Annu Rev Pathol 8: 49-78, 2013.
8. Sekaran V, Soares J and Jarstfer MB: Telomere maintenance as a target for drug discovery. J Med Chem 57: 521-538, 2014.
9. Thomas SJ, Snowden JA, Zeidler MP and Danson SJ: The role of JAK/STAT signalling in the pathogenesis, prognosis and treatment of solid tumours. Br J Cancer 113: 365-371, 2015.
10. Furtek SL, Backos DS, Matheson CJ and Reigan P: Strategies and approaches of targeting STAT3 for cancer treatment. ACS Chem Biol 11: 308-318, 2016.
11. Koliaraki V, Pasparakis M and Kollias G: IKKβ in intestinal mesenchymal cells promotes initiation of colitis-associated cancer. J Exp Med 212: 2235-2251, 2015.
12. Li Y and Tergaonkar V: Noncanonical functions of telomerase: Implications in telomerase-targeted cancer therapies. Cancer Res 74: 1639-1644, 2014.
13. Hoesel B and Schmid JA: The complexity of NF-κB signaling in inflammation and cancer. Mol Cancer 12: 86, 2013.
14. Wang GW, Lv C, Shi ZR, Zeng RT, Dong XY, Zhang WD, Liu RH, Shan L and Shen YH: Abieslactone induces cell cycle arrest and apoptosis in human hepatocellular carcinomas through the mitochondrial pathway and the generation of reactive oxygen species. PLoS One 9: e115151, 2014.
15. Correia C, Lee SH, Meng XW, Vincelette ND, Knorr KL, Ding H, Nowakowski GS, Dai H and Kaufmann SH: Emerging understanding of Bcl-2 biology: Implications for neoplastic progression and treatment. Biochim Biophys Acta 1853: 1658-1671, 2015.
16. Lunardi S, Muschel RJ and Brunner TB: The stromal compartments in pancreatic cancer: Are there any therapeutic targets? Cancer Lett 343: 147-155, 2014.
17. Grivennikov SI and Karin M: Dangerous liaisons: STAT3 and NF-kappaB collaboration and crosstalk in cancer. Cytokine Growth Factor Rev 21: 11-19, 2010.
18. Wang XH, Liu BR, Qu B, Xing H, Gao SL, Yin JM, Wang XF and Cheng YQ: Silencing STAT3 may inhibit cell growth through regulating signaling pathway, telomerase, cell cycle, apoptosis and angiogenesis in hepatocellular carcinoma: Potential uses for gene therapy. Neoplasma 58: 158-171, 2011.
19. Barneda-Zahonero B and Parra M: Histone deacetylases and cancer. Mol Oncol 6: 579-589, 2012.
20. Li Z and Zhu WG: Targeting histone deacetylases for cancer therapy: From molecular mechanisms to clinical implications. Int J Biol Sci 10: 757-770, 2014.
21. Bhaskara S and Hiebert SW: Role for histone deacetylase 3 in maintenance of genome stability. Cell Cycle 10: 727-728, 2011.
22. Helleday T, Petermann E, Lundin C, Hodgson B and Sharma RA: DNA repair pathways as targets for cancer therapy. Nat Rev Cancer 8: 193-204, 2008.
23. Bhaskara S, Knutson SK, Jiang G, Chandrasekharan MB, Wilson AJ, Zheng S, Yenamandra A, Locke K, Yuan JL, Bonine-Summers AR, *et al*: Hdac3 is essential for the maintenance of chromatin structure and genome stability. Cancer Cell 18: 436-447, 2010.
24. Danial NN: BAD: Undertaker by night, candyman by day. Oncogene 27 (Suppl 1): S53-S70, 2008.
25. Bolden JE, Shi W, Jankowski K, Kan CY, Cluse L, Martin BP, MacKenzie KL, Smyth GK, Johnstone RW: HDAC inhibitors induce tumor-cell-selective pro-apoptotic transcriptional responses. Cell Death Dis 4: e519, 2013.
26. Gialeli C, Theocharis AD and Karamanos NK: Roles of matrix metalloproteinases in cancer progression and their pharmacological targeting. FEBS J 278: 16-27, 2011.
27. Frankowski H, Gu YH, Heo JH, Milner R and Del Zoppo GJ: Use of gel zymography to examine matrix metalloproteinase (gelatinase) expression in brain tissue or in primary glial cultures. Methods Mol Biol 814: 221-233, 2012.
28. Leinonen T, Pirinen R, Bohm J, Johansson R and Kosma VM: Increased expression of matrix metalloproteinase-2 (MMP-2) predicts tumour recurrence and unfavourable outcome in non-small cell lung cancer. Histology and histopathology 23: 693-700, 2008.

29. Lee H, Kim JS and Kim E: Fucoidan from seaweed Fucus vesiculosus inhibits migration and invasion of human lung cancer cell via PI3K-Akt-mTOR pathways. PLoS One 7: e50624, 2012.
30. Wang Z, Zhu S, Shen M, Liu J, Wang M, Li C, Wang Y, Deng A and Mei Q: STAT3 is involved in esophageal carcinogenesis through regulation of Oct-1. Carcinogenesis 34: 678-688, 2013.
31. Connelly L, Barham W, Onishko HM, Sherrill T, Chodosh LA, Blackwell TS and Yull FE: Inhibition of NF-kappa B activity in mammary epithelium increases tumor latency and decreases tumor burden. Oncogene 30: 1402-1412, 2011.
32. Haybaeck J, Zeller N, Wolf MJ, Weber A, Wagner U, Kurrer MO, Bremer J, Iezzi G, Graf R, Clavien PA, *et al*: A lymphotoxin-driven pathway to hepatocellular carcinoma. Cancer Cell 16: 295-308, 2009.
33. Fan Y, Mao R and Yang J: NF-κB and STAT3 signaling pathways collaboratively link inflammation to cancer. Protein Cell 4: 176-185, 2013.
34. West AC and Johnstone RW: New and emerging HDAC inhibitors for cancer treatment. J Clin Invest 124: 30-39, 2014.
35. Song X, Wang J, Zheng T, Song R, Liang Y, Bhatta N, Yin D, Pan S, Liu J, Jiang H, *et al*: LBH589 Inhibits proliferation and metastasis of hepatocellular carcinoma via inhibition of gankyrin/stat3/akt pathway. Mol Cancer 12: 114, 2013.
36. Lin TY, Fenger J, Murahari S, Bear MD, Kulp SK, Wang D, Chen CS, Kisseberth WC and London CA: AR-42, a novel HDAC inhibitor, exhibits biologic activity against malignant mast cell lines via down-regulation of constitutively activated Kit. Blood 115: 4217-4225, 2010.
37. Chien W, Lee DH, Zheng Y, Wuensche P, Alvarez R, Wen DL, Aribi AM, Thean SM, Doan NB, Said JW, *et al*: Growth inhibition of pancreatic cancer cells by histone deacetylase inhibitor belinostat through suppression of multiple pathways including HIF, NFκB, and mTOR signaling in vitro and in vivo. Mol Carcinog 53: 722-735, 2014.
38. He G and Karin M: NF-κB and STAT3 - key players in liver inflammation and cancer. Cell Res 21: 159-168, 2011.
39. Carpenter RL and Lo HW: STAT3 target genes relevant to human cancers. Cancers (Basel) 6: 897-925, 2014.
40. Song L, Rawal B, Nemeth JA and Haura EB: JAK1 activates STAT3 activity in non-small-cell lung cancer cells and IL-6 neutralizing antibodies can suppress JAK1-STAT3 signaling. Mol Cancer Ther 10: 481-494, 2011.
41. Jeannot V, Busser B, Vanwonterghem L, Michallet S, Ferroudj S, Cokol M, Coll JL, Ozturk M and Hurbin A: Synergistic activity of vorinostat combined with gefitinib but not with sorafenib in mutant KRAS human non-small cell lung cancers and hepatocarcinoma. Onco Targets Ther 9: 6843-6855, 2016.
42. Hanahan D and Weinberg RA: Hallmarks of cancer: The next generation. Cell 144: 646-674, 2011.
43. Low KC and Tergaonkar V: Telomerase: Central regulator of all of the hallmarks of cancer. Trends Biochem Sci 38: 426-434, 2013.
44. Sharma V, Koul N, Joseph C, Dixit D, Ghosh S and Sen E: HDAC inhibitor, scriptaid, induces glioma cell apoptosis through JNK activation and inhibits telomerase activity. J Cell Mol Med 14: 2151-2161, 2010.
45. Li CT, Hsiao YM, Wu TC, Lin YW, Yeh KT and Ko JL: Vorinostat, SAHA, represses telomerase activity via epigenetic regulation of telomerase reverse transcriptase in non-small cell lung cancer cells. J Cell Biochem 112: 3044-3053, 2011.
46. Kim JS, Lee SC, Min HY, Park KH, Hyun SY, Kwon SJ, Choi SP, Kim WY, Lee HJ and Lee HY: Activation of insulin-like growth factor receptor signaling mediates resistance to histone deacetylase inhibitors. Cancer Lett 361: 197-206, 2015.
47. Lee SC, Min HY, Jung HJ, Park KH, Hyun SY, Cho J, Woo JK, Kwon SJ, Lee HJ, Johnson FM, *et al*: Essential role of insulin-like growth factor 2 in resistance to histone deacetylase inhibitors. Oncogene 35: 5515-5526, 2016.
48. Min HY, Lee SC, Woo JK, Jung HJ, Park KH, Jeong HM, Hyun SY, Cho J, Lee W, Park JE, *et al*: Essential role of DNA methyltransferase 1-mediated transcription of insulin-like growth factor 2 in resistance to histone deacetylase inhibitors. Clin Cancer Res 23: 1299-1311, 2017.
49. Ceccacci E and Minucci S: Inhibition of histone deacetylases in cancer therapy: Lessons from leukaemia. Br J Cancer 114: 605-611, 2016.
50. Chen JB, Chern TR, Wei TT, Chen CC, Lin JH and Fang JM: Design and synthesis of dual-action inhibitors targeting histone deacetylases and 3-hydroxy-3-methylglutaryl coenzyme A reductase for cancer treatment. J Med Chem 56: 3645-3655, 2013.